Journal of Alloys and Compounds 509 (2011) 3223–3228

Contents lists available at ScienceDirect

Journal of Alloys and Compounds

journal homepage: www.elsevier.com/locate/jallcom

Evolution of structural and optical properties in the course of thermal evolution of sol–gel derived cobalt-doped gahnite

S. Kurajica[a,*], E. Tkalčec[a], B. Gržeta[b], D. Iveković[c], V. Mandić[a], J. Popović[b], D. Kranzelić[a]

[a] University of Zagreb, Faculty of Chemical Engineering and Technology, Marulićev trg 19, HR-10000 Zagreb, Croatia
[b] Division of Materials Physics, Ruđer Bošković Institute, Bijenička 54, HR-10000 Zagreb, Croatia
[c] University of Zagreb, Faculty of Food Technology and Biotechnology, Pierottijeva 6, HR-10000 Zagreb, Croatia

ARTICLE INFO

Article history:
Received 5 November 2010
Received in revised form 9 December 2010
Accepted 12 December 2010
Available online 22 December 2010

Keywords:
Transition metals compounds
Sol–gel process
Optical properties
Light absorption and reflection

ABSTRACT

Thermal evolution of sol–gel derived gahnite ($ZnAl_2O_4$) with 4, 8 and 12 at.% of Zn replaced with Co was studied by thermal analysis techniques (DTA/TGA), X-ray diffraction (XRD) and UV–vis diffuse reflectance spectroscopy (DRS). Zinc–cobalt spinel powders were produced by gel heat treatment at temperatures as low as 400 °C. Crystal structure was characterized using Rietveld refinement of X-ray diffraction patterns for the samples annealed at 800 °C, simultaneously with the analysis of diffraction line broadening. It was found out that the distribution of Co^{2+} ions in tetrahedral and octahedral sites of zinc cobalt aluminate crystal lattice, crystallite size and lattice strain depend on Co loading. The green color of samples thermally treated at $T < 800$ °C has been explained as a consequence of partial oxidation of Co^{2+} ions at lower temperatures and accommodation of Co^{3+} ions in octahedral sites. Thermal treatment at higher temperatures promote gradual change of color from green to blue, characteristic for tetrahedrally coordinated Co^{2+} ions. The spectra evolution could be interpreted as a progressive reduction of Co^{3+} to Co^{2+} ions at higher temperatures.

1. Introduction

Majority of blue ceramic pigments are based on cobalt ion, and one of most common crystalline material used for this purpose is cobalt aluminate ($CoAl_2O_4$). This intense blue color pigment, known as Thénard blue is characterized by its thermal and chemical stability, and also by its stability to solar exposure and atmospheric agents [1]. Beside ceramic, it is widely used for the coloration of plastics, paint, fibers, paper, rubber, glass and cement [1]. Cobalt and its salts are widely considered to be toxic and environmentally hazardous substances. The scarcity of Co and its difficult metallurgy make the use of cobalt raw materials expensive [2]. In order to minimize the use of cobalt in the preparation of blue ceramic pigments, the zinc aluminate, $ZnAl_2O_4$ (known by mineral name gahnite), proves to be a convenient host lattice allowing the development of intense blue colors with small amounts of cobalt ions substituting for zinc ions [3]. Zinc is considerably more abundant in nature and much less toxic than cobalt. Thus, partial replacement of cobalt by zinc in gahnite, producing of $(Zn,Co)Al_2O_4$ solid solutions can reduce the negative health, environmental, sustainability and economic considerations [2].

Both, zinc aluminate and cobalt aluminate have a normal spinel-type structure of the general formula AB_2O_4. Spinels crystallize in the cubic system, space group $Fd\bar{3}m$. The unit cell of the normal spinel structure contains 32 O^{2-} anions, 8 divalent cations A^{2+} in 8 tetrahedral interstices (of 64 available), and 16 trivalent cations B^{3+} in 16 octahedral interstices (of 32 available). On the other hand, the unit cell of the ideal inverse spinel structure contains 32 O^{2-} anions, 8 divalent cations A^{2+} in the octahedral interstices, while 16 trivalent cations B^{3+} are evenly divided between tetrahedral and octahedral interstices. Spinels can also possess some degree of cation disorder, which Verwey and Hellmann [4] described by introducing an inversion parameter, δ. This parameter is defined as a fraction of trivalent cation B^{3+} on tetrahedral cation site. The majority of spinels show some degree of cation disorder. Any intermediate partly disordered state may be expressed as a mixture of these two end members (the ideal normal spinel and the ideal inverse spinel, respectively) with a general formula $^{IV}[A_{1-\delta}\ B_{\delta}]\ ^{VI}[B_{2-\delta}A_{\delta}]\ O_4$, where δ is the inversion parameter.

Different chemical processing methods are used for the preparation of spinels [5] such as solid state reaction, co-precipitation, hydrothermal, combustion, sol–gel, etc. Compared with other techniques, the sol–gel method is a useful and attractive technique for the preparation of nanocrystalline materials for advanced technological applications, because it enables production of pure, homogeneous and ultra fine powders at low temperatures and

* Corresponding author. Tel.: +385 1 4597 281; fax: +385 1 4597 260.
E-mail address: stankok@fkit.hr (S. Kurajica).

0925-8388/$ – see front matter © 2010 Elsevier B.V. All rights reserved.
doi:10.1016/j.jallcom.2010.12.099

Table 1
Selected structural parameters for samples GC04, GC08 and GC12 heat treated at 800 °C resulted from Rietveld structure refinement.

Sample	Atom site	Occupancy [8]	δ [8]	Crystallite size (nm)	Lattice strain (%)
GC04	^{IV}A	0.003 Co + 0.96 Zn + 0.037 Al	0.037(4)	22.3	0.04
	^{VI}B	0.0185 Co + 0.9815 Al			
GC08	^{IV}A	0.029 Co + 0.92 Zn + 0.051 Al	0.051(3)	21.6	0.05
	^{VI}B	0.0255 Co + 0.9745 Al			
GC12	^{IV}A	0.065 Co + 0.88 Zn + 0.055 Al	0.055(4)	20.3	0.08
	^{VI}B	0.0275 Co + 0.9725 Al			

short calcinations times [6]. The use of nanoparticles can improve the pigment performance enhancing tribological and mechanical properties [7]. Another effect of nanoparticles, being smaller than the wavelengths of visible spectrum, is that no scattering and no reflection occur in the visible-light range, so the nanocomposite is transparent [7].

In this work nanoparticles of $(Zn,Co)Al_2O_4$ spinel pigment were prepared by sol–gel method. Samples were prepared in which 4, 8 and 12 at.% of zinc in the gahnite lattice was replaced with cobalt with the aim to obtain a blue ceramic pigment having reduced negative environmental impact and lower production costs.

2. Material and methods

2.1. Sample preparation

Three gels with composition $Zn_{1-x}Co_xAl_2O_4$, where $x = 0.04, 0.08, 0.12$ (denoted as GC04, GC08 and GC12, respectively) were prepared. For the preparation of gels the chelating agent ethyl-acetoacetate, $C_6H_{10}O_3$ (99%, Fluka, Germany), was firstly added to the sec-butanol, ^{s}BuOH (99%, Kemika, Croatia), and then the appropriate amount of aluminium sec-butoxide, $Al(O^sBu)_3$ (97%, Aldrich, Great Britain), was firstly dissolved in the ^{s}BuOH/$C_6H_{10}O_3$ solution. $Al(O^sBu)_3$ was added to the solution using syringe to minimize exposure to air humidity. The appropriate amounts of zinc nitrate hexahydrate, $Zn(NO_3)_2{\cdot}6H_2O$ (99%, Kemika, Croatia), and cobalt nitrate hexahydrate, $Co(NO_3)_2{\cdot}6H_2O$ (99%, Kemika, Croatia), were also dissolved in ^{s}BuOH. Both solutions were stirred for 1 h before the nitrate salts solution was added drop wise to the $Al(O^sBu)^3/C_6H_{10}O_3$ solution. The molar ratio of $Al(O^sBu)_3$:$C_6H_{10}O_3$:[$Zn(NO_3)_2{\cdot}6H_2O$ + $Co(NO_3)_2{\cdot}6H_2O$]:^{s}BuOH was 2:2:1:10. The mixture was stirred in a closed reactor for 24 h at room temperature. No precipitation was observed during that period. The clear red-colored sols were poured into a large Petri dish in order to maximize exposure to air moisture and kept at room temperature. After 2 days the gelation occurred and completely transparent gels were obtained. Drying of the gels for five more days at room temperature enabled the evaporation of solvent and the release of alkoxy groups resulting in a dry product. The obtained samples were then subsequently grinded to fine powders. The powders were heated in the furnace with static air at a heating rate of 10 °C/min and calcined at various temperatures between 200 and 900 °C for 2 h. Afterwards they were slowly cooled to RT in the furnace. The prepared samples were denoted GC04, GC08 and GC12 (Table 1).

2.2. Characterization

The thermal behavior of powder precursors was characterized by differential thermal analysis (DTA) and thermo-gravimetric analysis (TGA) using a simultaneous DTA/TGA analyzer Netzsch STA 409. For the thermal analysis ~50 mg of material were placed in Pt crucibles and heated at a rate of 10 °C min^{-1}.

Crystalline phases formed by thermal treatment of the samples were identified by powder X-ray diffraction (XRD) using a Philips MPD 1880 diffractometer with monochromatized CuKα radiation. Diffraction patterns for phase identification were collected between 5° and 70° 2θ in steps of 0.02° and with a fixed counting time of 2 s per step. The samples that were heat treated at 800 °C were additionally scanned in the 2θ range from 10° to 140°, in steps of 0.02°(2θ) with fixed counting time of 7 s per step, for the purpose of structure refinement and line broadening analysis by the Rietveld method. Rietveld method was performed by the program X'Pert HighScore Plus, version 2.1 (PANalytical 2004using a pseudo-Voigt profile function and the polynomial background model. The instrumental line broadening was determined using silicon powder (Koch-Light Lab. Ltd., 99.999% purity, spherical particles with diameter of 1 μm).

UV–vis diffuse reflectance spectra (DRS) of the samples were acquired using an OceanOptics USB 2000 spectrometer equipped with a bifurcated fiber-optic reflection probe. Spectroscopically pure barium sulphate was used as a reference and matrix for sample dilution. Reflectance data were recorded between 300 and 800 nm with a spectral resolution of 0.2 nm. A total of 50 spectra were collected per sample and averaged to increase the signal-to-noise ratio. The measured reflectance data were transformed to Kubelka-Munk function using equation $F(R) = (1-R)^2/2R$, where R is reflectance of the sample.

3. Results and discussion

3.1. Thermal behavior of the dried gels

Fig. 1 shows DTA and TGA curves of the as-prepared gels. Several thermal features took place during the heating of the gels. A wide endotherm in the range between room temperature and ~160 °C, sharp exotherm at ~160 °C and two more exotherms, between 250 and 350 °C as well as between 600 and 700 °C are seen on DTA curve. TG curves show four weight loss steps: a continuous loss of ~18% between room temperature and ~160 °C, a rapid weight loss of 23–31% at ~160 °C followed by weight loss of 15–18% between 180 and 330 °C. An additional small continuous loss at temperatures higher than 300 °C could also be seen on TG curves.

Based on our previous detailed investigation on gahnite synthesis using the sol–gel technique [5] the peaks in DTA-TGA curves could be assigned as follows: the first endothermic DTA peak, accompanied by continuous weight loss seen on TGA curves of the samples (Fig. 1), was induced by evaporation of the residual solvent and physically adsorbed water from the gel. The sharp exothermic peak at ~160 °C on DTA curves of samples accompanied with rapid weight loss is a consequence of an auto-combustion process involving nitrates and organic phase. Weight loss between 180 °C and 300 °C could be attributed to formation of nitrous gasses due to decomposition of nitrates. The peaks in the temperature range 250–350 °C and 600–700 °C indicate crystallization processes. It seems that under dynamic heat-treatment the spinel phase crystallizes in two steps. The two-steps crystallization processes seen on DTA scans can be explained with the fact that the majority of zinc and cobalt content is not at disposal for reaction until the end of nitrate decomposition process.

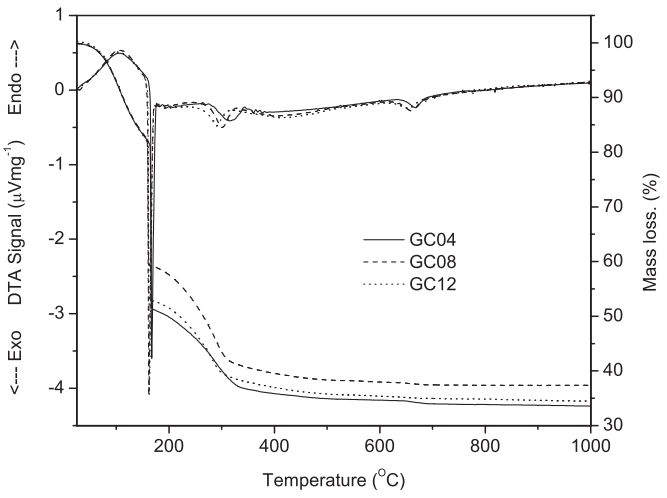

Fig. 1. DTA and TGA patterns of samples GC04, GC08 and GC12.

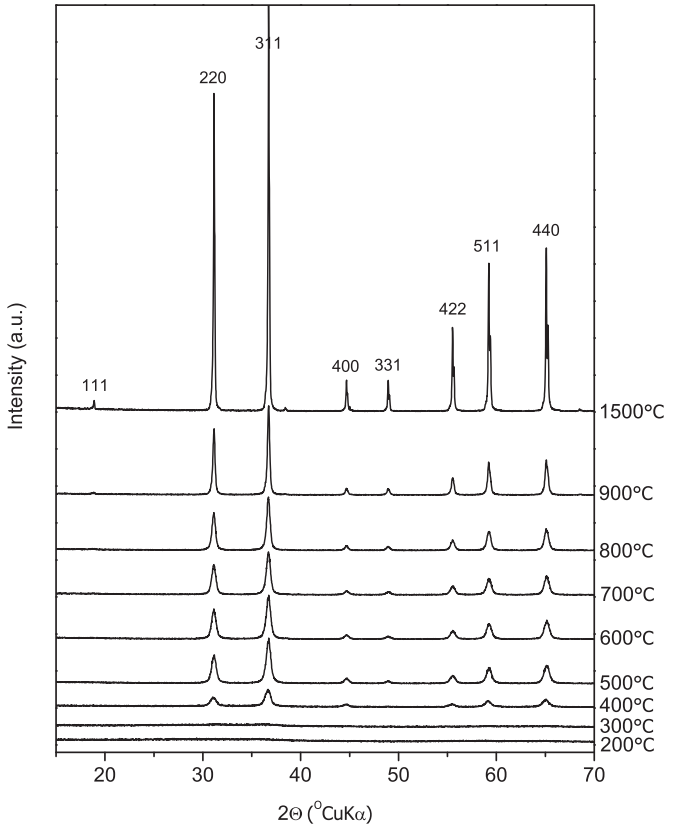

Fig. 2. X-ray powder diffraction patterns of the sample GC12 calcined at various temperatures. The patterns have been vertically displaced for clarity.

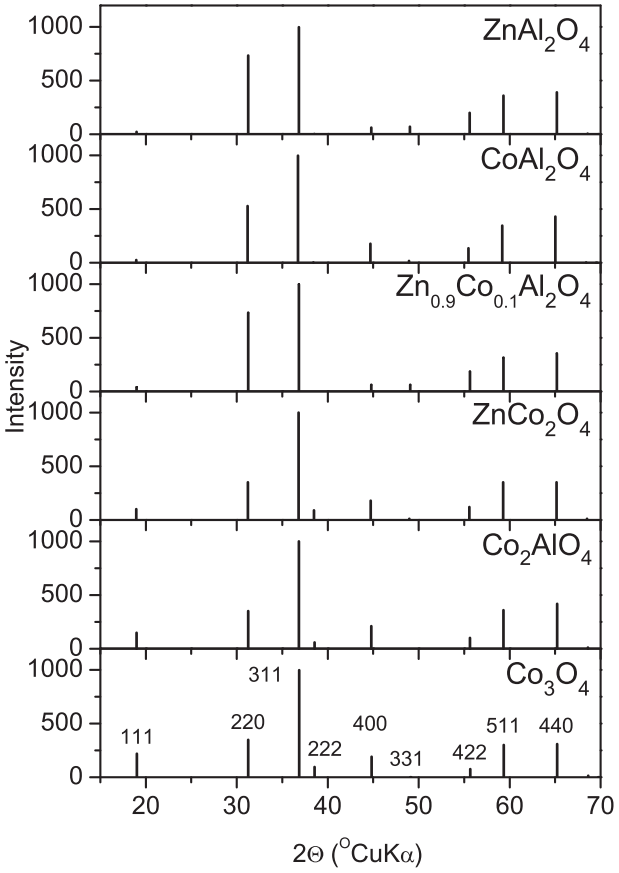

Fig. 3. Graphical representation of PDF data for $ZnAl_2O_4$ (82-1043), $CoAl_2O_4$ (82-2252), $Zn_{0.9}Co_{0.1}Al_2O_4$ (76-0070), $ZnCo_2O_4$ (23-1390), Co_2AlO_4 (38-814), Co_3O_4 (74-2120).

3.2. Phase evolution and structural analysis of heat-treated samples

Samples were heat-treated at various temperatures between 200 °C and 1500 °C and subtracted to XRD diffraction. XRD patterns of sample GC12 are given in Fig. 2 as example. Samples heat treated below 400 °C are completely XRD amorphous. At 400 °C very broad peaks of low intensity centered at 31.2°, 36.8°, 44.7°, 55.6°, 59.3° and 65.2° 2θ attributed to cubic spinel-type structure appear. None of the samples heated up to higher temperatures yielded other phase beside spinel-type phase. With the increase of thermal treatment temperature the peak intensity increases, but the position of the peaks and their relative intensities remain unchanged. This is true even for the samples heat treated at 1500 °C.

For the purpose of phase identification in the collected XRD patterns of samples, the patterns listed in the powder diffraction database for the following phases were taken into consideration: $ZnAl_2O_4$ (82-1043), $CoAl_2O_4$ (82-2252), $ZnCo_2O_4$ (23-1390), Co_2AlO_4 (38-814), Co_3O_4 (74-2120), as well as double aluminates (e.g. $Zn_{0.9}Co_{0.1}Al_2O_4$, 76-0070). All these phases have the spinel-type structure, very close value of lattice parameter *a*, and similar XRD patterns (Fig. 3).

The differentiation between $ZnAl_2O_4$, $CoAl_2O_4$ and $Zn_{0.9}Co_{0.1}Al_2O_4$ on one side and $ZnCo_2O_4$, Co_2AlO_4 andCo_3O_4 on the other side could be made from the relative intensity of diffraction peak 222. The 222 reflection at 38.5°2θ is significantly stronger for phases belonging to second group, while it appears with very small intensity or is absent from XRD patterns of phases belonging to the first group of proposed phases, respectively (Fig. 3). On the basis of absence of (222) reflection (Fig. 2), regardless of heat treatment temperature except 1500 °C, it could be concluded that none of phases from the second group is present in the samples. The intensities in the XRD patterns of prepared samples are most consistent with zinc cobalt aluminate, $Zn_{0.9}Co_{0.1}Al_2O_4$ (card no. 76-0070).

In our previous work [8] it was shown that samples of Co-doped gahnite heat-treated at 800 °C for 2 h were single-phase spinel samples with partially inverse spinel structure. All the above mentioned phases were considered in the course of refinement. Except for the case of zinc cobalt aluminate, the scale factor for these phases dropped to zero almost instantly. Therefore, it could be claimed with certainty that the samples thermally treated at 800 °C have no additional phases. The inversion parameter increased with increasing Co content in gahnite. At a low Co-doping level the portion of Co on octahedral sites is a large part of total Co content (almost 93% of total Co content in sample GC04). The portion of Co on octahedral sites decreases to 61% and 46 of total Co content for samples GC8 and GC12, respectively. According to Zayat and Levy, [9] oxidative conditions during the formation of the spinel phase could lead to higher degree of inversion in the Co–Al spinel structure.

As seen in Fig. 2, the increase of heat-treatment temperature caused the increase in intensities of diffraction lines, and decrease in their full-widths at half-maximum (FWHM), indicating on crystallites growth in the samples during the heat treatment.

The broad diffraction lines of samples heat treated at lower temperatures indicated nano-crystalline nature of the samples, and no anisotropy of diffraction line broadening was noticed. The crystallite dimension in spinel-type material is of fundamental importance for its properties as coloring agent. When such material is in a form of micron-sized pigment, it is opaque, having good hiding power. On the other hand, when it is in the form of nano-sized

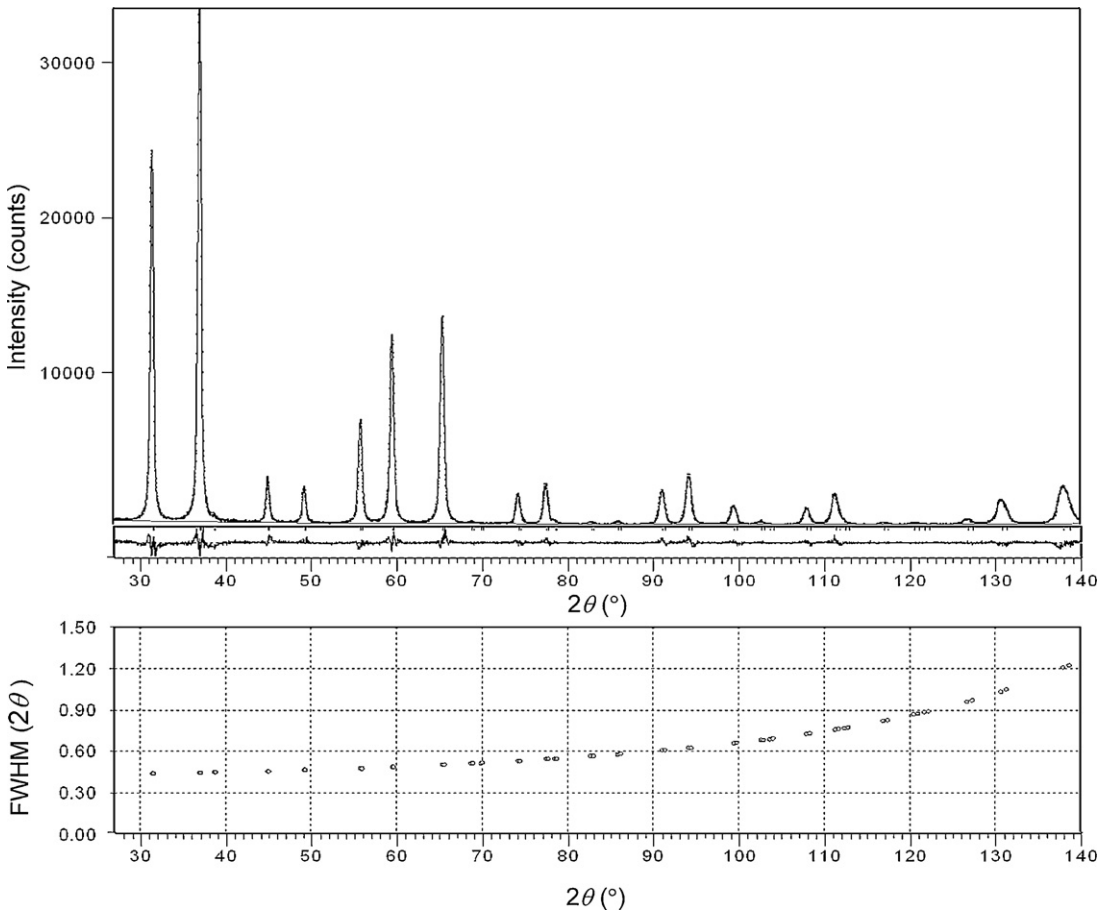

Fig. 4. Rietveld refinement and size-strain analysis of sample GC8 calcined at 800 °C for 2 h.

pigment dispersed in a matrix, it exhibits transparency along with color generation [1].

Therefore, in the present work the Rietveld method for diffraction line broadening analysis of samples thermally treated at 800 °C has been performed. The observed and calculated powder XRD patterns for sample GC08 are presented in Fig. 4 along with the values of full-widths at half-maximum (FWHM) in the wide range of Bragg angle. Table 1 presents some results of structure refinement and results of line broadening analysis performed by the Rietveld refinement for samples heat-treated at 800 °C for 2 h. Line broadening was caused by both small crystallite sizes and lattice strain. The crystallite sizes decreased with the increase in cobalt doping level, from 22.3 nm for sample doped with 4 at.% Co to 20.3 nm for sample doped with 12 at.% Co. In such manner the nano-crystalline nature of spinel particles in investigated samples is confirmed. The lattice strain increased from 0.04% for sample doped with 4 at.% Co to 0.08% for 12 at.% Co. Such behavior can be explained by the fact that introducing of dopand ions (Co^{2+}) into the gahnite structure causes the increases of lattice strain.

3.3. Color evolution and UV–vis analyses of heat-treated samples

Dried powder samples before the heat treatment were pink due to presence of cobalt nitrate in the samples, which suggested that cobalt ions did not undergo any oxidation process and existed as Co^{2+} species in the octahedral sites [10]. Thermal treatment changed the colors of the samples; from the starting pink color to light grey (200–300 °C), then to green (400–700 °C), where intensity of green color increased with temperature, and finally to light-blue color (800–900 °C), also showing some increase in intensity with temperature. The increase in intensities of green and blue color of the samples (at the appropriate temperature) with Co loading was noted too.

The occurrence of an intense blue color is not a surprise because many common cobalt pigments, cobalt aluminate being one of them, are intense blue due to electronic transitions of Co^{2+} in tetrahedral coordination [11]. On the other hand, the occurrence of green color is associated with electronic transitions of Co^{3+} in octahedral coordination [11], i.e. it points out to a partial oxidation of Co^{2+} to Co^{3+} species [10]. Zayat and Levy also noted greenish colored sol–gel derived $CoAl_2O_4$ films at the annealing temperature below 700 °C and concluded that the annealing temperature and stoichiometry play an important role in their coloration [9]. The influence of preparation route on temperature at which the color of the samples changes from green to blue has also been observed [9,12]. The oxidizing environment produced during thermal decomposition of the nitrates could promote oxidation of cobalt to Co^{3+} ion [6,13] and the existence of Co^{3+} ions in octahedral coordination may lead to a development of green coloration [14].

In order to further investigate the structural characteristics of the samples, UV–vis DRS spectra of samples annealed at different temperatures were analyzed. DRS spectra of samples GC04, GC08, and GC12 heat-treated at temperatures between 100 and 900 °C are shown in Fig. 5. The spectra of all three samples exhibit similar features. Samples annealed at 100 °C show absorption only at wavelengths shorter than 400 nm due to the presence of cobalt (II) nitrate. In the spectra of samples annealed at higher temperatures, two broad absorption bands appear in the wavelength ranges 320–420 nm and 520–660 nm, along with two low-intensity

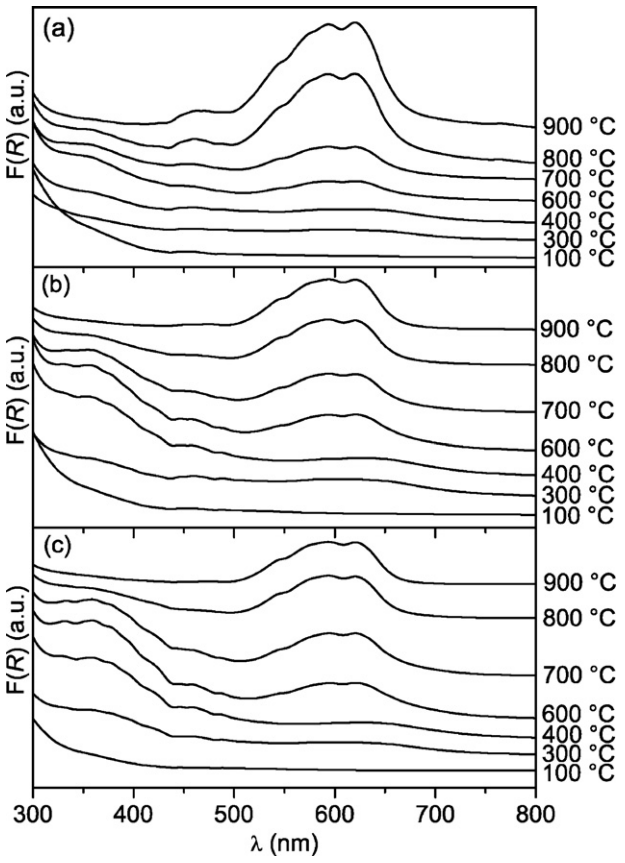

Fig. 5. UV–vis diffuse reflectance spectra of samples (a) GC04, (b) GC08, and (c) GC12, annealed at different temperatures. Spectra are shifted along the *y*-axis for clarity.

absorption bands centered at ca. 460 nm and 660 nm, the later being heavily overlapped with the band that appears in the 520–660 nm range. The absorption band in the wavelength range 320–420 nm and the low-intensity absorption band at 660 nm can be attributed to the $^1A_{1g} \rightarrow {}^1T_{2g}$ and $^1A_{1g} \rightarrow {}^1T_{1g}$ transitions, respectively, of octahedrally coordinated low-spin Co^{3+} ions [10,15,16]. The absorption band that appears between 520 and 660 nm has multiplet structure with major maxima at 545, 595 and 620 nm, and it can be assigned to the $^4A_2(F) \rightarrow {}^4T_1(P)$ transition of tetrahedrally coordinated Co^{2+} ions in the spinel structure of $CoAl_2O_4$ [17–19]. The band splitting may be attributed to a low symmetry perturbation, which lifts the degeneracy of the $^4T_1$ excited levels, a dynamic Jahn–Teller effect due to the distortion of tetrahedral structure, or to a spin–orbit coupling [20]. Finally, a low-intensity absorption band centered at 460 nm can be attributed to the symmetry forbidden $^4T_{1g}(F) \rightarrow {}^4T_{1g}(P)$ transition of octahedrally coordinated Co^{2+} ions in the spinel structure [17,18]. Thus, the DRS spectra of samples reveal the presence of Co^{3+} ions in octahedral coordination, as well as the presence of tetrahedrally and octahedrally coordinated Co^{2+} ions.

The evolution of DRS spectra with the increase of sample heat-treatment temperature is in accordance with the conclusions drawn in previous two chapters. Partial oxidation of Co^{2+} ions to the Co^{3+} ions, caused by the thermal decomposition of nitrate ions at temperatures between 180 and 300 °C, [13] leads to the appearance of the Co^{3+} absorption bands in the DRS spectra of samples (band in the wavelength range 320–420 nm and band at 660 nm, Fig. 5). Due to the absorption in blue and red part of the visible spectrum caused by these bands, the samples annealed in the temperature range between 300 and 700 °C exhibit greenish hue [21]. The intensities of these two absorption bands did not change significantly with the increase of temperature in the range 400–700 °C. However, at temperatures higher than 700 °C, a rapid decrease in the intensity of Co^{3+} absorption bands in DRS spectra of all three samples was observed (Fig. 5). This effect can be attributed to the reduction of Co^{3+} to Co^{2+}, which is a thermodynamically favored process at temperatures higher than 700 °C [1,9]. Samples annealed at 900 °C show no absorption in the wavelength range between 320 and 420 nm (Fig. 5), indicating that all Co^{3+} ions were reduced to Co^{2+} ions at this temperature.

From the spectra shown in Fig. 5 it is evident that the decrease of intensity of the absorption bands associated with octahedrally coordinated Co^{3+} ions is accompanied with the simultaneous increase of intensities of the absorption bands associated with the Co^{2+} ions. The intensity of the triplet band assigned to tetrahedrally coordinated Co^{2+} ions continuously increased with the increase of calcination temperature, and this band became the most prominent band in the spectra of samples annealed at 800 °C. As a consequence, the color of samples changed from green to blue at 800 °C. A continuous increase of the intensity of absorption band attributed to octahedrally coordinated Co^{2+} ions (low-intensity band at 460 nm) with the increase of temperature has been observed for the sample GC04 (Fig. 5a). For the samples GC08 and GC12 (Fig. 5b and c), the intensity of the band at 460 nm increased with the increase of temperature up to 600 °C. With further increase of annealing temperature the intensity of the same band decreased.

The evolution of DRS spectra with temperature could be interpreted as follows: at lower temperatures polycrystalline zinc cobalt spinel crystallize, having at least a part of cobalt in Co^{3+} oxidation state accommodated in octahedral coordination. The increasing of annealing temperatures in air caused the progressive reduction to Co^{2+} causing change of color from green to blue.

The comparison of spectra of the samples GC04, GC08, and GC12 shown in Fig. 5 reveals that the formation of structural units with octahedrally coordinated Co^{3+} ions, as well as the distribution of Co^{2+} ions between the tetrahedral and octahedral sites of aluminate lattice, varies with the Co-loading of the samples. The absorption band that appears in the wavelength range 320–420 nm, attributed to the Co^{3+} ions in octahedral sites, is weak for the sample GC04 and increases in the intensity going from the sample GC04 to the sample GC12. This allows the conclusion that the number of structural sites with octahedrally coordinated Co^{3+} ions is the smallest in the sample GC04 and that it increases with the Co-loading of the samples. Additionally, the intensity ratio of the absorption band at 460 nm (assigned to octahedrally coordinated Co^{2+}) and the triplet band appearing between 520 and 660 nm (attributed to tetrahedrally coordinated Co^{2+}) decreases with the increase of Co-loading of the samples, indicating that the fraction of Co^{2+} ions occupying the octahedral lattice sites becomes smaller for the samples with higher Co-loading. This conclusion agrees well with the results of Rietveld refinement, which showed that the fraction of Co-ions occupying the octahedral positions is highest for the sample GC04 and lowest for the sample GC12. Even a large part of Co^{2+} ions is in octahedral sites (93, 61 and 46% of total Co content for samples GC04, GC08 and GC12, respectively) the color-decisive factor is fraction of Co^{2+} in tetrahedra. The reason for that is low absorption coefficient associated with this species [17]. The 460 nm $^4T_{1g}(F) \rightarrow {}^4T_{1g}(P)$ transition of octahedrally coordinated Co^{2+} ions is almost two orders of magnitude weaker than the $^4A_2(F) \rightarrow {}^4T_1(P)$ transition of tetrahedrally coordinated Co^{2+} ions [18].

4. Conclusion

Thermal evolution of gahnite doped with small amounts of cobalt, prepared by sol–gel process, was studied.

Spinel-type phase was obtained by prolonged treatment at temperatures as low as 400 °C. Spinels prepared at 800 °C display a presence of Co^{2+} ions in tetrahedral and octahedral coordination and have crystallite size between 20.3 and 22.3 nm and lattice strain between 0.04 and 0.08%.

In the course of thermal treatment at lower temperatures a partial oxidation of Co^{2+} to Co^{3+} occurs. The Co^{3+} ions are accommodated in octahedral sites causing the green appearance of samples. The heat treatment at temperature above 700 °C promoted the reduction of Co^{3+} ions and brought about the appearance of Co^{2+} ions in tetrahedral coordination, and change of color from green to blue. The appearance of Co^{3+} and Co^{2+} ions, as well the distribution of Co^{2+} cations in tetrahedral and octahedral sites of spinel-type structure, depended on cobalt doping level and heat-treatment temperature.

Acknowledgment

The financial support of the Ministry of Science, Education and Sports of Republic of Croatia within the framework of the projects nos. 125-1252970-2981 and 098-0982886-2893 is gratefully acknowledged.

References

[1] G. Carta, M. Casarin, N. El Habra, M. Natali, G. Rossetto, C. Sada, E. Tondello, P. Zanella, Electrochim. Acta 50 (2005) 4592–4599.
[2] A. Forés, M. Llusar, J.A. Badenes, J. Calbo, M.A. Tena, G. Monrós, Green Chem. 2 (2000) 93–100.
[3] X. Duan, D. Yuan, Z. Sun, C. Luan, D. Pan, D. Xu, M. Lv, J. Alloys Compd. 386 (2005) 311–314.
[4] E.J.W. Vewey, E.L. Heilmann, J. Chem. Phys. 15 (1947) 174–180.
[5] S. Kurajica, E. Tkalcec, J. Sipusic, G. Matijasic, I. Brnardic, I. Simcic, J. Sol–Gel Sci. Technol. 46 (2008) 152–160.
[6] M. Zayat, D. Levy, J. Sol–Gel Sci. Technol. 25 (2002) 201–206.
[7] P.M.T. Cavalcante, M. Dondi, G. Guarini, M. Raimondo, G. Baldi, Dyes Pigments 80 (2009) 226–232.
[8] J. Popovic, E. Tkalcec, B. Grzeta, S. Kurajica, B. Rakvin, Am. Mineral. 94 (2009) 771–776.
[9] M. Zayat, D. Levy, Chem. Mater. 12 (2000) 2763–2769.
[10] M. Herrero, P. Benito, F.M. Labajos, V. Rives, J. Solid State Chem. 180 (2007) 873–884.
[11] F. Tielens, M. Calatayud, R. Franco, J.M. Recio, J. Pérez-Ramírez, C. Minot, Solid State Ionics 180 (2009) 1011–1016.
[12] F. Meyer, R. Hempelmann, S. Mathur, M. Veith, J. Mater. Chem. 9 (1999) 1755–1763.
[13] F. Yu, J. Yang, J. Ma, J. Du, Y. Zhou, J. Alloys Compd. 468 (2009) 443–446.
[14] X.H. Xu, F.X. Qin, F.X. Jiang, X.L. Li, Y. Chen, G.A. Gehring, Appl. Surf. Sci. 254 (2008) 4956–4960.
[15] Y. Brik, M. Kacimi, M. Ziyad, F. Bozon-Verduraz, J. Catal. 202 (2001) 118–128.
[16] I. Zacharaki, C.G. Kontoyannis, S. Boghosian, A. Lycourghiotis, Ch. Kordulis, Catal. Today 143 (2009) 38–44.
[17] L.F. Liotta, G. Pantaleo, A. Macaluso, G. Di Carlo, G. Deganello, Appl. Catal. A: Gen. 245 (2003) 167–177.
[18] J.Y. Yan, C.M. Kung, W.M.H. Sachtler, H.H. Kung, J. Catal. 172 (1997) 178–186.
[19] F.E. Trigueiro, C.M. Ferreira, J.-C. Volta, W.A. Gonzalez, P.G. Pries de Oliveria, Catal. Today 118 (2006) 425–432.
[20] A.A. Verberckmoes, B.M. Weckhuysen, R.A. Schoonheydt, Micropor. Mesopor. Mater. 22 (1998) 165–178.
[21] U. Lavrenčič-Štangar, B. Orel, M. Krajnc, R. Cerc Korošec, P. Bukovec, Mater. Technol. 36 (2002) 387–394.